

## MINERALS OF THE HOLLANDITE SUPERGROUP: CRYSTAL-CHEMISTRY AND THERMAL BEHAVIOR

CARMEN CAPALBO

Dipartimento di Scienze della Terra, Università di Pisa, Via Santa Maria 53, 56126 Pisa

The considerable interest in tunnel oxides arises from their technological importance related to their microporous features. Specifically, tunnel oxides are often referred to as Octahedral Molecular Sieves (OMS), an acronym that mirrors that of ZSM that is applied to zeolite-like molecular sieves. The latter are based on a tetrahedral framework. Thanks to the features in common with zeolites, tunnel oxides have the capability to incorporate extra-framework cations and therefore are used as cation exchangers, immobilization agents and catalysts (Whitney, 1975; Ringwood *et al.*, 1979; Lind & Hem, 1993; Prusty *et al.*, 1994; Ghoneimy, 1997; Randall *et al.*, 1998). Beside the many applications, tunnel oxides are very common in nature and are found in a wide variety of geological settings (Potter & Rossman, 1979; Post, 1999).

Among the tunnel oxides phases, we focused our interest on minerals of the hollandite supergroup, which are by far the most important and common. Structurally they are characterized by octahedral walls (2×2 octahedra wide) cross-linked to each other to build up a tunnel structure and these tunnels are large enough to host mono- and divalent cations (tunnel cations) and in some cases water molecules (Byström & Byström, 1950). On chemical grounds, the hollandite supergroup can be divided into two groups depending on the dominant tetravalent cation in the octahedral walls: the coronadite group (with Mn<sup>4+</sup> as octahedral cation) and the priderite group (with Ti<sup>4+</sup> as octahedral cation).

Several X-ray diffraction experiments at ambient and non-ambient conditions on several samples of hollandite *s.l.* minerals have been widely discussed, with the aim of better understanding the cation distribution within the tunnels as well as the thermal behavior of these minerals. A series of analyses carried out to ascertain the presence of water molecules in the tunnels has been performed. Moreover, the nomenclature revision as well as the new classification of minerals of hollandite supergroup has been presented.

The main outputs of the work are presented below.

As a general rule, a mineral is considered a distinct species on the basis of the dominant chemical element at any independent crystallographic site (Hatert & Burke, 2008). In this specific case, the nomenclature of the members of the hollandite supergroup, and their status as valid species, depend on both the dominant tunnel cation (A<sup>+</sup> or A<sup>2+</sup>, called DTC) and the dominant charge-compensating octahedral cation (M<sup>3+</sup>, or more rarely M<sup>2+</sup>, called DCCC) that partially substitutes for the tetravalent cation (Mn<sup>4+</sup> or Ti<sup>4+</sup>) in the octahedra.

The previous databases and lists of mineral species did not provide a clear identification of the DTC and DCCC, and for some of the minerals of the supergroup a clear definition of the end-member formula was lacking. As a consequence, minerals with different compositions were mentioned in literature with the same name. Therefore a new classification was necessary.

The main results of the new classification are the following:

- re-definition of hollandite as the Ba-Mn<sup>3+</sup> end-member of the coronadite group and concurrent introduction in the mineralogical nomenclature of ferrihollandite, the Ba-Fe<sup>3+</sup> end-member;
- discreditation of the mineral ankangite (= mannardite);
- definition of all the end-member formulae of all existing and potentially new mineral species of the hollandite supergroup.

In literature data of both natural and synthetic members of the supergroup, positional disorder at the tunnel cations positions is often observed (Sinclair *et al.*, 1980; Post *et al.*, 1982; Post & Burnham, 1984).

In fact the cations are displaced off the special positions [(0,0,0) or (0,0,½)] due to the different ionic radii and to the local interactions with the oxygen atoms of the framework, as well as to the impossibility of placing

cations on neighbour, translationally related and fully occupied sites, in two adjacent unit cells along the tunnel axis.

Most of our samples have shown the characteristic tunnel cations displacement as observed in many literature cases. Moreover, the samples follow the rule that when the tunnel sites are occupied by divalent A cations (such as  $\text{Ba}^{2+}$ ), the site occupancy is near 50% (*i.e.* 1.0 atoms per unit cell) whereas when the tunnel sites are occupied by monovalent cations (such as  $\text{K}^+$ ) then the site occupancy is near 66% (*i.e.* 1.33 atoms per unit cell) (Post & Bish, 1989). This corresponds respectively to two main types of sequences of filling the tunnel A sites:

- 1) A1 – □ (occupancy  $\approx$  50%);
- 2) A2a – A2b – □ (occupancy  $\approx$  66%).

Among the samples studied, there are three cryptomelanes,  $[\text{K}(\text{Mn}^{4+}_7\text{Mn}^{3+})\text{O}_{16}]$ , two hollandites *s.s.*,  $[\text{Ba}(\text{Mn}^{4+}_6\text{Mn}^{3+}_2)\text{O}_{16}]$ , three ferrihollandites,  $[\text{Ba}(\text{Mn}^{4+}_6\text{Fe}^{3+}_2)\text{O}_{16}]$ , and one mannardite,  $[\text{Ba}(\text{Ti}^{4+}_6\text{V}^{3+})\text{O}_{16}]$ . Almost all the samples were refined with a single cell (*c* or *b* axis  $\approx$  2.9 Å), space group *I4/m* or *I2/m*, but two samples of ferrihollandite (from Kājilidongri and Vagli) which were refined with a double cell (*b* axis  $\approx$  5.8 Å, space group *P2/n*).

The samples with  $\text{K}^+$  as dominant tunnel cation showed approximately a tunnel occupancy of 66%. In fact, as EMPA data and structural refinement showed, cryptomelane from Montalto di Mondovì  $[(\text{K}_{1.06}\text{Ba}_{0.15}\text{Sr}_{0.12}\text{Na}_{0.04})_{\Sigma=1.37}(\text{Mn}^{4+}_{6.43}\text{Mn}^{3+}_{0.83}\text{Fe}^{3+}_{0.69}\text{Al}^{3+}_{0.03}\text{Zn}^{2+}_{0.01}\text{Mg}^{2+}_{0.01})_{\Sigma=8}\text{O}_{16}]$  has respectively 1.37-1.40 atom per unit cell, indicating that the sequence A2a – A2b – □, with  $\frac{2}{3}$  of tunnel sites filled, is the most probable.

Cryptomelane from Sitapur mine  $[(\text{K}_{1.04}\text{Na}_{0.24}\text{Sr}_{0.18}\text{Ba}_{0.12})_{\Sigma=1.58}(\text{Mn}^{4+}_{6.35}\text{Mn}^{3+}_{1.25}\text{Fe}^{3+}_{0.22}\text{Al}^{3+}_{0.11})_{\Sigma=7.93}\text{O}_{16}]$  has 1.58 (from EMPA data) and 1.12 (from structural refinement) atoms per unit cell, indicating that both sequences above described are possible. Also in cryptomelane from Kājilidongri mine (no chemical analyses are available) the probability to find both the two tunnel sequences is almost the same.

All the other samples have  $\text{Ba}^{2+}$  as dominant tunnel cation. All of them have less than 1.33 atoms per unit cell (from structural refinements and from EMPA data), therefore the A1 – □ sequence (tunnel occupancy of 50%) is the most likely to occur.

Another issue addressed in this work has been the structural study of hollandite *s.l.* minerals at non ambient conditions, particularly at low and high temperature, aiming at understanding the effect of temperature on the cation mobility and the distortions that these minerals may undergo.

Single-crystal X-ray diffraction measurements were performed on ferrihollandite from Vagli and from Kājilidongri (ideally  $\text{BaMn}^{4+}_6\text{Mn}^{3+}_2\text{O}_{16}$ , *s.g.* *P2/n*), and mannardite from Monte Arsiccio (ideally  $\text{BaTi}^{4+}_6\text{V}^{3+}_2\text{O}_{16}$ , *s.g.* *I4/m*) in the range of temperature from 100 to 900 K. At room temperature ferrihollandite and mannardite are topologically very similar: mannardite has ideal topological symmetry *I4/m*, *a* = 10.142 (1), *c* = 2.9533 (3), whereas ferrihollandite framework is slightly distorted and assumes monoclinic structure, *P2/n*, *a* = 10.006 (6), *b* = 5.746 (1), *c* = 9.796 (3) Å,  $\beta$  = 90.75(2)°.

As expected, with increasing temperature the unit cell volume as well as interatomic distances of both phases increase quite regularly. However, a substantial difference between the thermal behaviors of the two minerals has been observed.

Monoclinic ferrihollandite (*P2/n*) undergoes a transition to pseudo-tetragonal (*P4/m*, *a* = 9.915 (2), *b* = 5.764 (2), *c* = 9.904 (5) Å,  $\beta$  = 90.08°) at 530 K. This reaction is reversible for an heating up to 530 K. Above this temperature the transition to the tetragonal form becomes irreversible.

Conversely, mannardite is tetragonal (*I4/m*) within the whole T range (from 100 to 800 K) and does not undergo any structural transition.

Complete structural refinements of ferrihollandite and mannardite from low T ( $T_{\min}$  = 100 K) to high T ( $T_{\max}$  = 1000 K) revealed an interesting mobility of the tunnel cations at varying the temperature.

In both samples the structural refinement revealed the presence of two Ba sites, Ba1 and Ba2.

In ferrihollandite at LT and RT conditions the occupancy of Ba1 sites ( $\approx 80\%$ ) is higher than that of Ba2 ( $\approx 20\%$ ). Increasing the T up to 1000 K the opposite situation is observed: the occupancy of Ba2 site ( $\approx 60\%$ ) is greater than that of Ba1 ( $\approx 40\%$ ). This trend suggests that, if we had the possibility to reach higher temperature, all barium would concentrate in the Ba2 site whereas the Ba1 would become empty.

In mannardite, the opposite behavior has been observed. At LT and RT condition both sites Ba1 and Ba2 are partially occupied ( $\approx 75\%$  and  $\approx 35\%$  respectively). At higher temperature, 500 and 700 K, all barium tends to concentrate in the Ba1 site (100%) and Ba2 site becomes empty.

Taking into account the substantial differences between the two thermal behaviors of ferrihollandite and mannardite, a comparison of the variation of the unit cell parameters with T has been done in both cases. The aim was to observe the different elasticity of the structures as a function of temperature (Fig. 1).

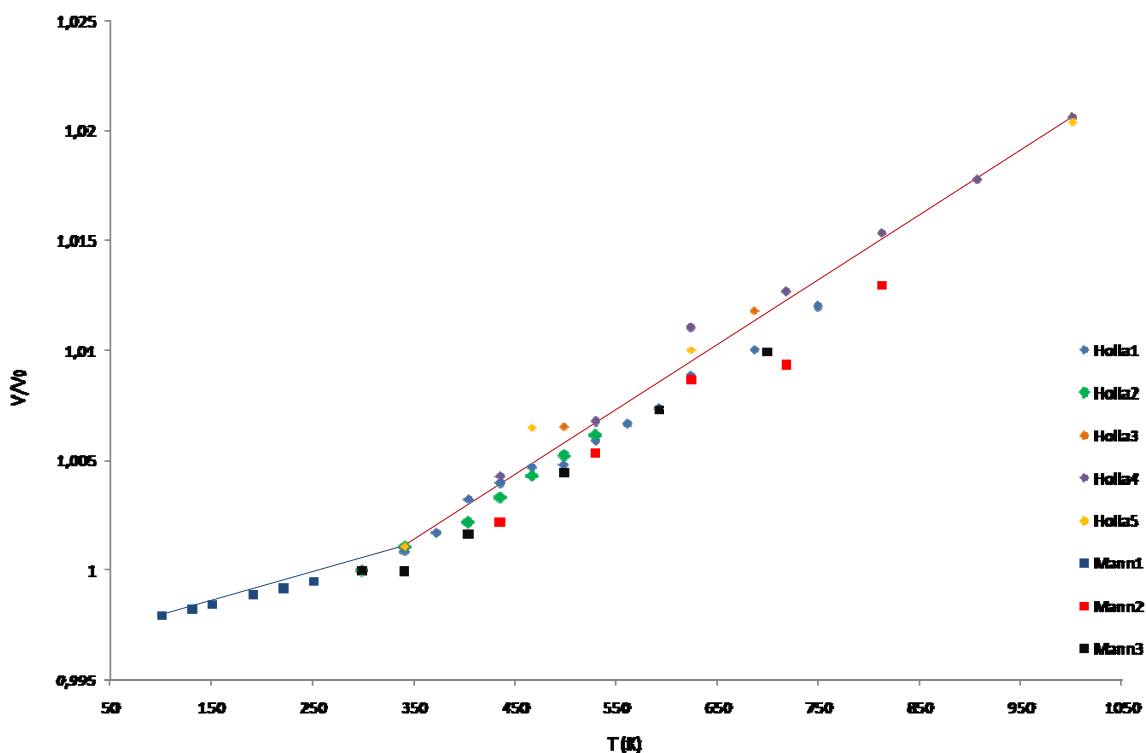


Fig. 1 -  $V/V_0$  for ferrihollandite and mannardite at different temperatures. The volume data are normalized with respect to the room-temperature. The rhombs symbols represent different specimens of ferrihollandite, the square symbols represent mannardite samples.

In spite of the observed differences, ferrihollandite and mannardite have the same structural rigidity, increasing the temperature. Analytical points (plotted in Fig. 1) follow the same trend. Unfortunately, no LT data for ferrihollandite have been recorded. We may only assume that the same trend of mannardite could be valid for ferrihollandite, too. Different angular coefficients, that correspond to the volumetric thermal expansion coefficient  $\alpha_V$ , are observed in the LT-RT and RT-HT portions (Table 1). The volumetric thermal expansion coefficients have been calculated through the formula  $\alpha_V = 2 \times [(V_{HT} - V_{RT}) / (V_{HT} + V_{RT})] / (HT - RT)$  for T range from 298 K to 1000 K, and through the formula  $\alpha_V = 2 \times [(V_{RT} - V_{LT}) / (V_{RT} + V_{LT})] / (RT - LT)$  for T range from 100 K to 150 K (calculated only for mannardite sample), where  $V_{HT}$ ,  $V_{RT}$ ,  $V_{LT}$  are the volume values at 1000, 298, and 100 K respectively. For  $100 < T$  (K)  $< 298$  the structure is more rigid in respect to temperature variations: in the LT region of the diagram the volumetric thermal expansion coefficient  $\alpha_V$  is three-times lower if compared to that calculated for the HT region.

Table 1 - Volumetric thermal expansion coefficients  $\alpha_V$  for ferrihollandite and mannardite in respect to temperature variations.

T (K)	$\alpha_V$ (mannardite)	$\alpha_V$ (ferrihollandite)
100 < T < 298	$10.4 \times 10^{-6}$	-
298 < T < 1000	$25.11 \times 10^{-6}$	$29.10 \times 10^{-6}$

Finally we aimed at defining the possible presence of water in the minerals of the hollandite supergroup. In fact, due to the microporous nature of these minerals, it cannot be excluded that the tunnels may host water molecules as well.

In order to ascertain the presence of H<sub>2</sub>O molecules in hollandite minerals, TG/DSC and IR analyses, as well as a study through a modeling approach, have been performed on samples of ferrihollandite from Vagli and mannardite from Monte Arsiccio.

Through the modelling approach we tried to include water molecules in the tunnels of the two minerals in place of the barium sites. This would avoid the unlikely Ba...Ba interactions between neighbour cations. In both “hydrous” models the  $R_F$  decreased, although slightly, in respect to the  $R$  observed for “anhydrous” models (from 5.01% to 4.97% for ferrihollandite, and from 2.20% to 2.06% for mannardite).

The improvement of the  $R_F$  values of both ferrihollandite and mannardite is too low to allow us to decide which of the two models (anhydrous and hydrous) better fits the experimental data, anyway it cannot be excluded that ferrihollandite from Vagli and mannardite from Monte Arsiccio contain some water molecules into the tunnels. Essentially, what we obtained for both structures is a coordination polyhedron of the Ba sites formed by eight oxygen atoms and two water molecules. The interatomic distances Ba-O and Ba-H<sub>2</sub>O are more than acceptable.

In order to confirm the presence of H<sub>2</sub>O molecules, TG/DSC runs have been carried out for ferrihollandite from Vagli.

According to the TGA results we observed that the possible water desorption, corresponding to a weight loss of about 0.4%, ends below about 550 °C. Subsequently, three weight losses of about 1.8, 3 and 4% were observed. These latter weight losses were related to the oxygen loss that occurs with reduction of Mn<sup>4+</sup> in ferrihollandite, leading to the formation of oxygen-deficient products such as bixbyite [(Mn<sup>3+</sup>,Fe<sup>3+</sup>)<sub>2</sub>O<sub>3</sub>] and hausmannite (Mn<sup>2+</sup>Mn<sup>3+</sup><sub>2</sub>O<sub>4</sub>).

To confirm the TGA results, one sample of ferrihollandite from Vagli and two sample of mannardite, from Monte Arsiccio and Rough Claims, have been analyzed by IR spectroscopy.

For ferrihollandite from Vagli, IR spectroscopy did not reveal any peak relative to the OH<sup>-</sup> stretching vibration: this could indicate that the sample of ferrihollandite is anhydrous, or that the water content is too low to be detected.

On the contrary, for both mannardite samples the strongest absorption peaks appeared in the 2500-3700 cm<sup>-1</sup> region, with positions at *ca.* 3350 and 3500 cm<sup>-1</sup>. These values correspond to the OH<sup>-</sup> stretching vibrations of hydrogen-bonded water molecules. A rather broad H<sub>2</sub>O bending band of lower intensity is present in both samples at about 1600 cm<sup>-1</sup>. This indicates that there are some water molecules in the mannardite samples.

Thanks to this last analysis, we can confirm that the mineral previously known as ankangite (the current mannardite from Monte Arsiccio) is chemically identical to mannardite minerals, even in the water content.

Moreover we can confirm that a small amount of “zeolitic water” may often be present in minerals of the hollandite supergroup.

## REFERENCES

Byström, A. & Byström, A.M. (1950): The crystal structure of hollandite, the related manganese oxides minerals and  $\alpha$ -MnO<sub>2</sub>. *Acta Crystallogr.*, **B34**, 146-154.

- Ghoneimy, H.F. (1997): Adsorption of CO<sub>2</sub>-type hydrous manganese-dioxide (and Zn<sup>2+</sup> on cryptomelane). *J. Radioanal. Nucl. Chem.*, **223**, 61-65.
- Hatert, F. & Burke, E.A.J. (2008): The IMA-CNMNC dominant-constituent rule revisited and extended. *Can. Mineral.*, **46**, 717-728.
- Lind, C.J. & Hem, J.D. (1993): Manganese minerals and associated fine particulates in the streambed of Pinal Creek, Arizona, U.S.A.; a mining-related acid drainage problem. *Appl. Geochem.*, **8**, 67-80.
- Post, J.E. (1999): Manganese oxides minerals: crystal structures and economic and environmental significance. *Proc. Nat. Acad. Sci. USA*, **96**, 3447-3454.
- Post, J.E. & Burnham, C.W. (1984): Disorder in high albite: insights from electrostatic energy minimizations. *Geol. Soc. Am. Abstr.*, **16**, 625.
- Post, J.E. & Bish, D.L. (1989): Rietveld refinement of the coronadite structure. *Am. Mineral.*, **74**, 913-917.
- Post, J.E., Von Dreele, R.B., Buseck, P.R. (1982): Symmetry and cation displacement in hollandites: structure refinement of hollandite, cryptomelane and priderite. *Acta Crystallogr.*, **B38**, 1056-1065.
- Potter, R.M. & Rossman, G.R. (1979): The tetravalent manganese oxides: identification, hydration, and structural relationship by infrared spectroscopy. *Am. Mineral.*, **64**, 1199-1218
- Prusty, B.G., Sahu, K.C., Godgul, G. (1994): Metal contamination due to mining and milling activities at the Zawar zinc mine, Rajasthan, India. 1. Contamination of stream sediments. *Chem. Geol.*, **112**, 275-292.
- Randall, S.R., Sherman, D.M., Ragnarsdottir, K.V. (1998): An extended X-ray absorption fine structure spectroscopy investigation of cadmium sorption on cryptomelane (KMn<sub>8</sub>O<sub>16</sub>). *Chem. Geol.*, **151**, 95-106.
- Ringwood, A.E., Kesson, S.E., Ware, N.G., Hibberson, W., Major, A. (1979): Immobilization of high level nuclear reactor wastes in SYNROCK. *Nature*, **278**, 219-233.
- Sinclair, W., McLaughlin, G.M., Ringwood, A.E. (1980): The structure and chemistry of a barium titanate hollandite-type phase. *Acta Crystallogr.*, **36**, 2913-2918.
- Whitney, P.R. (1975): Relationship of manganese-iron oxides and associated heavy metals to grain size in stream sediments. *J. Geochem. Explor.*, **4**, 251-263.